Dalton Transactions

Accepted Manuscript

This article can be cited before page numbers have been issued, to do this please use: M. Sethuraman, T. Khamrang, M. Velusamy and M. Ramasamy, *Dalton Trans.*, 2017, DOI: 10.1039/C7DT03062B.

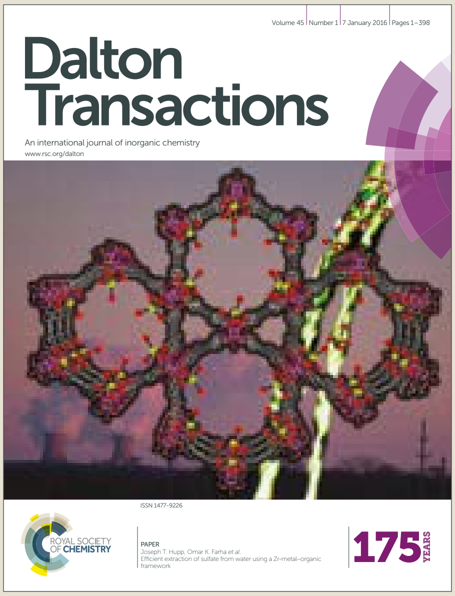

Volume 45 | Number 1 | 7 January 2016 | Pages 1–398

Dalton Transactions

An international journal of inorganic chemistry
www.rsc.org/dalton

ISSN 1477-9226

ROYAL SOCIETY OF CHEMISTRY

PAPER
Joseph T. Hupp, Omar K. Farha et al.
Efficient extraction of sulfate from water using a Zr-metal–organic framework

175 YEARS

ROYAL SOCIETY OF CHEMISTRY

rsc.li/dalton

View Article Online
DOI: 10.1039/C7DT03062B

Dalton Transactions

ARTICLE

Catalytic fixation of atmospheric carbon dioxide by copper(II) complexes of bidentate ligands

Received 00th January 20xx,
Accepted 00th January 20xx

DOI: 10.1039/x0xx00000x

www.rsc.org/

Sethuraman Muthuramalingam,[a] Themmila Khamrang,[b] Marappan Velusamy,*[, b] and Ramasamy Mayilmurugan*[,a]

New copper(II) complexes $[Cu(L1)_2(H_2O)](ClO_4)_2$, **1** [L1 = 2-pyridin-2-yl-quinoline], $[Cu(L2)_2(H_2O)](ClO_4)_2$, **2** [L2 = 2-pyridin-2-yl-quinoxaline], $[Cu(L3)_2(H_2O)](ClO_4)_2$, **3** [L3 = 6,7-dimethyl-2-pyridin-2-yl-quinoxaline], $[Cu(L4)_2(H_2O)](ClO_4)_2$, **4** [L4 = 4-phenyl-2-pyridin-2-yl-quinoline] and $[Cu(L5)_2(H_2O)](ClO_4)_2$, **5** [L5 = 4-phenyl-2-pyridin-2-yl-quinazoline] were synthesized and characterized as the catalysts for selective fixation of atmospheric CO_2. The molecular structure of **2** was determined by single-crystal X-ray studies and showed unusual trigonal bipyramid geometry (τ, 0.936) around copper(II) center by the coordination of two ligand units and a water molecule. The $Cu–N_{quin}$ (2.040, 2.048 Å) bonds are slightly longer than $Cu–N_{pyr}$ (1.987 Å) bonds but shorter than $Cu\text{-}O_{water}$ bond (2.117 Å). A well-defined Cu(II)/Cu(I) redox potentials around 0.352 to 0.401 V were observed for **1** - **5** in acetonitrile solution. The electronic absorption spectra of **1** - **5** showed ligand-based transitions around 208 -286 nm with a shoulder around 342 - 370 nm. The d-d transitions appeared around 750 - 800 and 930-955 nm in acetonitrile. The rhombic EPR spectra of **1 - 5** have exhibited three different g values g_x, 2.27-2.34; g_y, 2.06 - 2.09; g_z, 1.95 - 1.98 at 70 K. The atmospheric CO_2 has been fixed successfully by **1** - **5** using Et_3N as sacrificial reducing agent and afforded the CO_3^{2-} bound complexes of type $[Cu(L)CO_3(H_2O)]$, which are accomplished by an absorption band around 614 - 673 nm and ν_{st} at 1647 cm^{-1}. This CO_3^{2-} bound complex of **1** has been crystallized from the reaction mixture and it showed distorted square pyramidal geometry (τ, 0.369) around copper(II) center via the coordination of only one ligand unit, a carbonate, and water molecules. Further, the treatment of one equivalent H^+ with carbonate bounded Cu(II) complexes have liberated bicarbonate (HCO_3^-) and regenerated parent complexes under N_2 atmosphere. The regenerated catalysts were active enough to fix the CO_2 for eight repeating cycles without any change in the efficiency. The fixation of CO_2 is possibly proceeds via the formation of Cu(I)-species accomplished by the MLCT band around 450 - 500 nm. The rates of Cu(I)-species formation were determined as k_{obs}, 5.41 - 10.31 × 10^{-3} s^{-1} in the presence of Et_3N in acetonitrile at 25 °C. Interestingly, the copper(I)-species of **3** has been successfully crystallized and showed distorted tetrahedral geometry by the coordination of two units of ligand L3.

Introduction

The rising level of atmospheric CO_2 is well documented in the recent years due to the technological revolutions, which increase the combustion of fossil fuels, and has widespread environmental concerns. In recent decades, CO_2 capture and recycling have gained great attention and many efforts have developed to process the CO_2 emission. Exploring green and sustainable energy resources and devising efficient methods for CO_2 capture, sequestration and utilization are urgently required. One rational approach is to utilize CO_2 as C1-building block for synthesizing valuable compounds, due to the low cost and nontoxicity of CO_2.[1-7] Currently, carbon capture and storage/sequestration (CCS) from source point is one among the most promising strategies being implemented to reduce carbon emissions.[8-12] So far, four major methods, such as chemical, photochemical, electrochemical and enzymatic methods are exploited to catalyze the CO_2 fixation/conversion. In the first three methods, the low selectivity is often reported due to the stable form of the carbon element in the molecule of CO_2 and energetically difficult to acquire high catalytic performances. The fourth one though is the enzymatic method, which provides an eco-friendly and promising way for efficient CO_2 fixation/conversion because of its superior stereo-specificity and regio/chemo-selectivity.[1-6] In fact, metalloenzymes such as CO_2 fixing enzyme carbon monoxide dehydrogenase (CODH) is capable of both CO_2 to CO reduction and CO to CO_2 oxidation. The [Ni-4Fe-4S] core adopted by CODH active site to handle this redox-mediated interconversion. The zinc(II) containing carbonic anhydrase enzyme is catalyzing CO_2 to CO_3^{2-} conversion via non-redox pathway and D-ribulose and non-heme iron in the photosystem II are known to play crucial roles in the fixation and activation of CO_2.[13-20]

[a] *Bioinorganic Chemistry Laboratory/Physical Chemistry, School of Chemistry, Madurai Kamaraj University, Madurai 625021, Tamilnadu, India.*
Email; mayilmurugan.chem@mkuniversity.org
[b] *Department of Chemistry, North Eastern Hill University, Shillong 793022, India*

† Footnotes relating to the title and/or authors should appear here.

Electronic Supplementary Information (ESI) available: [details of any supplementary information available should be included here]. See DOI: 10.1039/x0xx00000x

View Article Online
DOI: 10.1039/C7DT03062B

Only a few bioinspired approaches have made to activate CO_2 and its fixation by using ecologically viable copper catalysts. Peacock and co-workers have reported the fixation of CO_2 as oxalate by copper(II) complexes of ligand *N,N′,N′′*-triallyl-1,4,7-triazacyclononane in 2001.[21] Later, Verdejo and co-workers showed that fixation of the CO_2 into carbonate by using copper(II) complexes of a terpyridinophane aza receptor in 2004.[22] Bouwman and co-workers have reported the selective conversion of atmospheric CO_2 into oxalate by electrochemical method using a dicopper(I) complex of *N*-(2-mercaptopropyl)-*N,N*-bis(2-pyridylmethyl)amine in 2010.[23] In 2014, Fujisawa and co-workers have reported the conversion of CO_2 into oxalate catalyzed by copper(II) complexes of hydrotris(3,5-diisopropyl-1-pyrazolyl)borate anion and non-innocent ligand α-keto acid.[24] Maverick and co-workers have reported the reduction of carbon dioxide into oxalate by using binuclear copper complex of *m*-xylene containing pyridyltriazole spacer type ligand in 2014.[25] Also, Comba and coworkers have reported the dicopper(II) complexes of pseudo-octapeptides, synthetic analogues of ascidiacyclamide and the patellamides ligands as models for carbonic anhydrase and the conversion of CO_2 into CO_3^{2-}.[26] The atmospheric CO_2 has been fixed as carbonato bridge in the copper(II) complexes of N4 ligands under basic conditions were reported by Mautner and co-workers in 2015.[27] Surprisingly, most of these studies were rarely fixed atmospheric CO_2 under a mild condition. Thus, we envisioned to develop simple copper complexes for CO_2 fixation under ambient condition and attempted to study their mechanism. In this article, we are reporting the synthesis and characterization of simple copper(II) complexes of bidentate ligands as the catalyst for fixation of atmospheric CO_2 under mild conditions. The molecular structures of one of the complexes and complex bridged with CO_3^{2-} originated from atmospheric CO_2 and key copper(I)-intermediate have been successfully characterized by single crystal X-ray studies. The fixation and kinetic studies have shown that fixation of atmospheric CO_2 is simultaneous and selective over other atmospheric gases. The present ligand architecture, donor properties of the heterocyclic nitrogen donors provide important differences to other related previously reported catalysts. Further, our ligands are able to adopt preferable tetrahedral coordination geometry for key copper(I) intermediate to fix carbon dioxide (cf. below). To the best of our knowledge, our report is the novel example of copper(II) complexes based on bidentate ligands for simultaneous fixation and sequestration of atmospheric carbon dioxide under mild condition.

Result and Discussion

The bidentate ligands L1 - L5 were synthesized by a one-pot condensation reaction by following literature methods with slight modifications (Scheme 1).[28-31] The quinoline-based ligands 2-pyridin-2-yl-quinoline (L1) and 4-phenyl-2-pyridin-2-yl-quinoline (L4) were prepared by Friedlander condensation reaction.[28,29] However, the quinoxaline based ligands 2-pyridin-2-yl-quinoxaline (L2), 6,7-dimethyl-2-pyridin-2-yl-quinoxaline (L3) were conveniently synthesized by using SiO_2 as a catalyst.[30] The quinazoline based ligand 4-phenyl-2-pyridin-2-yl-quinazoline (L5) was synthesized by the simple condensation of (2-amino-phenyl)-phenyl-methanone with pyridine-2-carbaldehyde.[31] All the ligands were characterized by ^1H NMR and ESI-MS spectral methods. The mononuclear copper(II) complexes of these ligands have been isolated by reacting two equivalents of the corresponding ligand with one equivalent of $Cu(ClO_4)_2{\cdot}6H_2O$ in methanol at room temperature (Scheme 1). The complexes were formulated as $[Cu(L)_2(H_2O)](ClO_4)_2$ (**1** - **5**) and their stoichiometry is further supported by single crystal X-ray structure of **2**. The HR-MS data reveals that the complexes are retaining their structures even in solution, **1**: *m/z*, 475.0989 for $C_{28}H_{20}CuN_4$ $[M]^+$; **2**: *m/z*, 477.0899 for $C_{26}H_{18}CuN_6$ $[M]^+$; **3**: *m/z*, 533.0563 for $C_{30}H_{26}CuN_6$ $[M]^+$; **4**: *m/z*, 627.1624 for $C_{40}H_{28}CuN_4$ $[M]^+$ and **5**: *m/z*, 629.1521 for $C_{38}H_{26}CuN_6$ $[M]^+$. This is also supported by values of molar conductivity in acetonitrile ($\Lambda M/\Omega^{-1}$ cm^2 mol^{-1}: 214-220), which falls in the range of 1:2 electrolytes.[32] The complexes **1** - **5** are moderately soluble in common organic solvents. The single crystals of **2** were grown from acetonitrile solution by slow diffusion of diethyl ether. The crystallization of other complexes was unsuccessful and yielded only the polycrystalline solids.

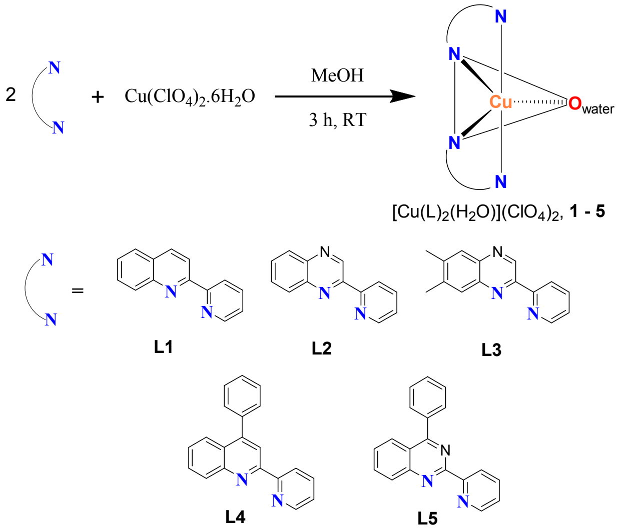

Scheme 1. Synthesis of Cu(II) complexes **1-5** of bidentate ligands.

Molecular structure of $[Cu(L2)_2(H_2O)](ClO_4)_2$ (2)

The single crystals of **2** have been crystallized in the space group of tetragonal I 41/a. The molecular structure of **2** along with donor atoms numbering scheme is presented in Figure 1 (Table 1 and 4). The structure of **2** adopts a trigonal bipyramid coordination geometry around copper(II) center, confirmed by the Addison parameter $\tau = 0.936$ ($\tau = \beta\text{-}\alpha/60$; $\beta = 177.3°$ and $\alpha = 121.1°$) which is zero and one for a square-pyramidal and trigonal bipyramidal geometries respectively.[33-35] The geometry is completed by nitrogen atoms of two ligand L2 units and one equatorially coordinated water molecule. Two quinoxaline nitrogen atoms N1 and N4 occupy the axial positions with the N1–Cu–N4 bond angle of 177.3°, which is higher than that of equatorial N3–Cu–N6 bond angle (121.1°) constituted by pyridine nitrogen donors and N6-Cu-

View Article Online
DOI: 10.1039/C7DT03062B

$O1_{water}$ bond angle (117.9°). Further, very slight distortion from ideal trigonal bipyramidal geometry has observed in equatorial bond angles of N3-Cu-N6 (121.1°), N6-Cu-O1 (117.9°) and N3-Cu-O1 (121.0°) from ideal trigonal bond angles (120°). The deviation of axial bond angle N1–Cu–N4 from ideal 180° is additionally confirming that slight distortion in the coordination geometry.[36] The $Cu–N_{quin}$ (2.040, 2.048 Å) bonds are slightly longer than $Cu–N_{pyr}$ (1.987 Å) bonds, which is reflected from the relatively stronger d-orbital overlapping of copper(II) with p-orbital of pyridine nitrogens than quinoxaline nitrogens. However, the observed $Cu-N_{py}/_{quin}$ bond distances and $Cu-O_{water}$ bond distance (2.117 Å) are in the range of those already reported for other trigonal bipyramidal copper(II) complexes containing analogues ligands.[37]

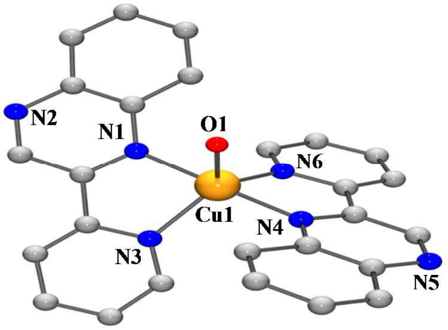

Figure 1. The molecular structure of $[Cu(L2)_2(H_2O)](ClO_4)_2$ **2** (Pov-ray figure drawn from 50% probability factor of thermal ellipsoids). The hydrogen atoms, H_2O molecule at outer coordination sphere and perchlorate counter ion are omitted for clarity.

Table 1. Selected bond distances[a] (Å) and bond angles[a] (°) for **2**.

Cu(1)-N(1)	1.987(4)
Cu(1)-N(3)	2.040(5)
Cu(1)-N(4)	1.987(4)
Cu(1)-N(6)	2.048(5)
Cu(1)-O(1)	2.117(5)
N(4)-Cu(1)-N(3)	100.16(18)
N(4)-Cu(1)-N(1)	177.3(2)
N(4)-Cu(1)-N(6)	80.72(19)
N(4)-Cu(1)-O(1)	88.4(2)
N(3)-Cu(1)-N(6)	121.1(2)
N(1)-Cu(1)-O(1)	88.93(19)
N(1)-Cu(1)-N(3)	81.44(19)
N(1)-Cu(1)-N(6)	100.16(18)
N(3)-Cu(1)-O(1)	121.0(2)
N(6)-Cu(1)-O(1)	117.9(2)

[a]Standard deviations in parenthesis

Electronic spectra

The absorption spectra of **1 - 5** displays d-d bands around 750 - 800 nm and 930 - 955 nm (Figure 2A, Table 2) in acetonitrile, originated from transitions $d_{xz} \approx d_{yz} \rightarrow d_{z^2}$ and $d_{xy} \approx d_{x^2-y^2} \rightarrow d_{z^2}$, which are being degenerate.[38,39] These spectral signatures are confirming the existence of five-coordinate geometry of copper(II) complexes in solution as similar to solid state. Very similar electronic spectral properties were reported for copper(II) complexes of pentacoordinate geometry.[39-43] The intense absorption bands were noticed in the ranges of 210-285 and 342 – 370 nm are assigned to intra ligand $n \rightarrow \pi^*$, $\pi \rightarrow \pi^*$ transitions. The energy of d – d transitions are following in the order of 776 (**1**) < 806 (**2**) > 802 (**3**) > 755 (**4)** < 785 (**5**) nm. The incorporation of additional nitrogen atom on the quinoline ring of **1** and **4** to obtain **2** and **5** respectively causing red-shift in the band position illustrating that the change in electronic nature of ligand by additional nitrogen atoms enhances the electron density on the aromatic rings.

The EPR spectra of **1** - **5** were rhombic in methanol: DMF (8:2) mixture at 70 K and exhibited three different g values. However, the EPR spectra were broad for all complexes in acetonitrile. The splitting of g-values in x, y and z-axis indicate that the geometry is in between the trigonal bipyramidal and square pyramidal geometries in cryogenic solution. Thus, the ground state is the linear combination of $d_{x^2-y^2}$ and d_{z^2} orbitals.[44] The predominance of the ground state level was calculated by $R = [(g_y - g_z)/(g_x - g_y)]$ within the g_x, g_y and g_z values.[45] The value R > 1 is indicating that the greater contribution from d_{z^2} orbital to the ground state and R < 1, the greater contribution to the ground state arises from $d_{x^2-y^2}$ orbital.[45] The complexes **1** - **5** exhibit almost similar values of g_x, (2.27 – 2.34) and the g_y and g_z values in the ranges of 2.06 – 2.09 and 1.95 – 1.98 respectively (Figure 2B, Table 2). The minor g-components reveal the presence of additional species, which are possibly originated from solvation, water exchange with anion or deprotonation. The large value of g_x is indicative of Cu-N bonds in more ionic nature and slight variations of the g_y and g_z values reflect in the geometrical distortion.[46,47] Further, the structure of the complexes appeared to be an elongated rhombus. The EPR spectrum of **1** appeared as rhombic with g_x (2.27) > g_y (2.07) > g_z (1.98) and R values of 0.61, which is suggesting the presence of $^2A_{1g}$ ground state with an unpaired electron on $d_{x^2-y^2}$ orbital.[48] The highest-energy half-occupied d-orbital being $d_{x^2-y^2}$ and its lobes pointing directly to the ligand orbitals with largest repulsive or antibonding interaction with the ligand field. The very similar trend in g values have also obtained for **2** – **5**, but the R-values are lower than **1**. Previously, a similar rhombic EPR spectral signatures with three different *g* values have been reported for five coordinate Cu(II) complexes $[Cu(phen)_2(H_2O)](NO_3)_2$ (phen=1,10-phenanthroline) and $[Cu(bpy)_2Cl]ClO_4$ (bpy = 2,2'-bipyridine). They showed R values of 2.14 and 1.54 respectively,[49] whereas $[Cu(phen)_2(H_2O)](BF_4)_2$ exhibited R values lower than 1 (0.73).[49] The geometry of these complexes was predicted as intermediate between the trigonal bipyramid and the square pyramid. The rhombic EPR spectra are different from the previously reported CuN_4 chromophores of the tetradentate ligands.[36] However, the rhombic EPR spectral signatures were reported for CuN_4 complexes of *N,N'*-dialkyl-1,10-phenanthroline-2,9-dimethanamine at higher pH values (8 - 10).[50]

View Article Online
DOI: 10.1039/C7DT03062B

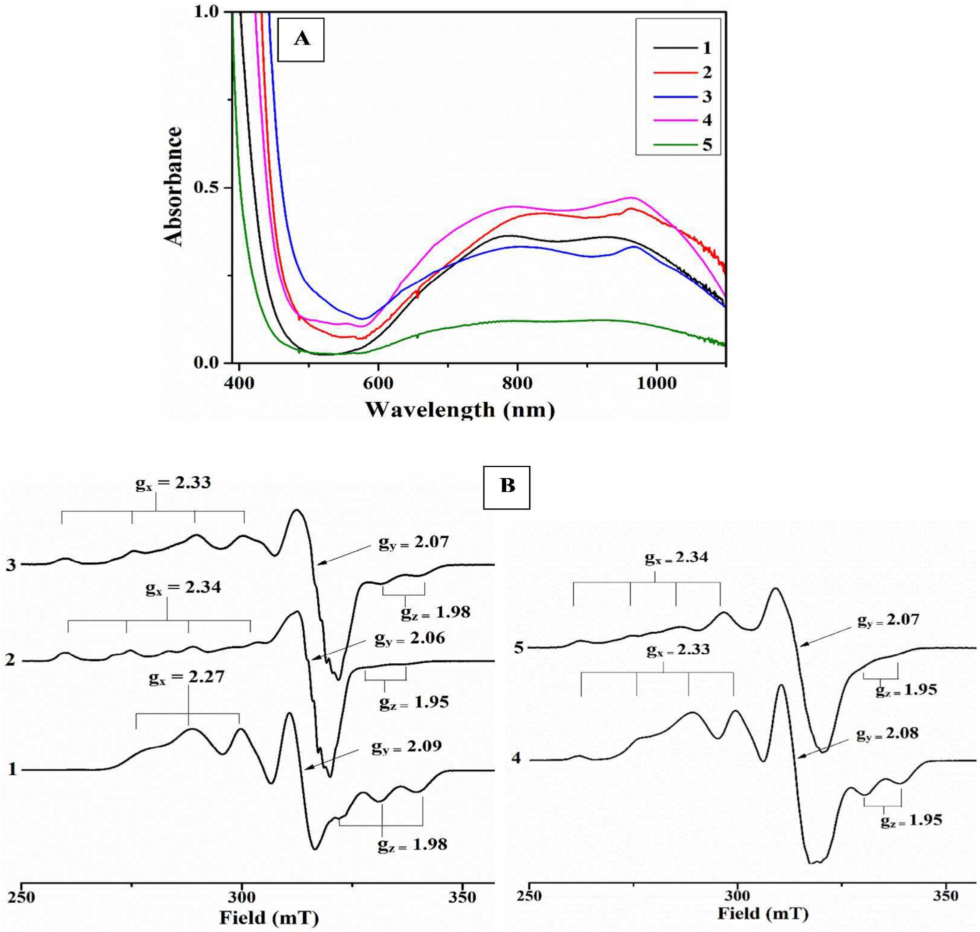

Figure 2. (A) Electronic absorption spectra of **1 - 5** in acetonitrile (1 × 10^{-3} M) at 25 °C. **(B)** EPR spectra for **1 – 5** in methanol:DMF (8:2) at 70 K and g-values are marked on each spectrum.

Redox Properties

The electrochemical behavior of **1 - 5** has studied by cyclic voltammetry (CV) under a nitrogen atmosphere at room temperature using 0.1 M tetrabutylammonium perchlorate (TBAP) as a supporting electrolyte in acetonitrile (Figure 3, Table 2). A platinum sphere/glassy carbon, a platinum wire, and Ag/Ag^+ were used as working, auxiliary and reference electrodes respectively.

The complex **1** exhibits cathodic ($Ep_{c,}$ 0.330 V) and anodic (E_{pa}, 0.450 V) waves with an irreversible Cu(II)/Cu(I) redox potential at 0.390 V. On replacing quinoline residue in **1** by quinoxaline and introducing additional methyl groups to obtain **2** and **3** respectively, showed an almost similar Cu(II)/Cu(I) redox potentials (**2**, 0.397; **3**, 0.401 V). This indicates that quinoxaline residue has no influence to modify

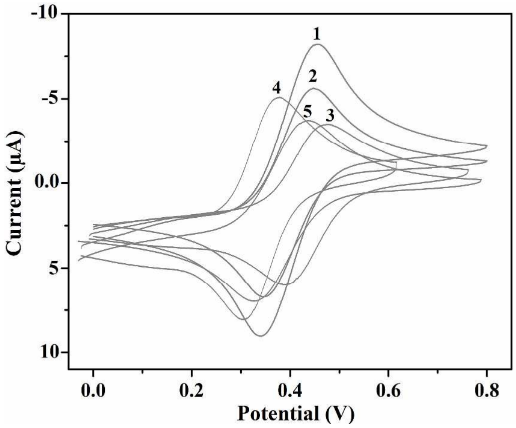

Figure 3. Cyclic voltammograms of complexes **1** - **5** (1 × 10^{-3} M) in acetonitrile at 25 °C. Supporting electrolyte: TBAP. Working electrode: Pt sphere, Reference electrode: Ag/Ag^+ (non-aqueous) and counter electrode: Pt wire.

View Article Online
DOI: 10.1039/C7DT03062B

Table 2. The electronic spectra, redox and kinetic data for **1 - 5**.

Compd.	Electronic Spectra[a]	EPR parameters[b]				IR data[e]	Redox data[c]				Kinetic data
	λ_{max}, nm (ε, M^{-1} cm^{-1})	g_x	g_y	g_z	R[d]	(cm^{-1})	Ep_a (V)	Ep_c (V)	ΔE (mV)	$E_{1/2}$ (V)	k_{obs} ($\times 10^{-3}$ s^{-1})[f]
1	943 (359), 776 (362) 342 (1698), 252 (3012) 208 (2850)	2.27	2.09	1.98	0.61		0.450	0.330	120	0.390	9.35 ± 0.005[g]
1a	614 (362)					1647	0.303	-121	424	0.090	6.22 ± 0.006[h]
2	954 (293), 806 (295) 359 (1774), 253 (2790)	2.34	2.06	1.95	0.39		0.449	0.346	103	0.397	8.72 ± 0.004[g]
2a	650 (295)					1653	0.272	-0.005	277	0.133	
3	949 (332), 802 (330) 370 (1686), 266 (1532)	2.33	2.07	1.98	0.34		0.44	0.362	78	0.401	10.31 ± 0.005[g]
3a	640 (330)					1647	0.210	0.077	133	0.143	
4	935 (541), 755 (550) 345 (1610), 278 (2578) 257 (2726)	2.33	2.08	1.95	0.52		0.422	0.282	140	0.352	5.41 ± 0.002[g]
4a	673 (550)					1649	0.278	0.023	255	0.151	
5	929 (214), 785 (215) 342 (696), 286 (1938) 251 (1552)	2.34	2.07	1.95	0.44		0.399	0.309	90	0.354	5.57 ± 0.006[g]
5a	643 (215)					1649	0.253	0.105	148	0.179	

[a] Concentration: 1×10^{-3} M in acetonitrile. [b] Measured at 70 K in methanol:DMF (8:2); $A_{||}$ and $A_{\perp}$ in 10^{-4} cm^{-1}. [c] Concentration: $1x10^{-3}$ M; supporting electrolyte: 0.1 M TBAP. [d] $R = [(g_{y}-g_{z)/(}g_{x}-g_{y})]$. [e] carbonate stretching frequency in **1a - 5a**. [f] k_{obs} = [1 + log(Abs)] vs time. [g] Formation of Cu(I)-species in acetonitrile. [h] Formation carbonate bound complex in acetonitrile.

Cu(II)/Cu(I) redox potentials and hence the Lewis acidity of copper(II) center. However, the ΔE values of **2** (103 mV) and **3** (78 mV) reveals that the switching of one electron Cu(II)/Cu(I) redox process from the irreversible into quasi-reversible. In contrast, the Cu(II)/Cu(I) redox potential of **4** and **5** are shifted to less positive redox potential (**4**, 0.352; **5**, 0.354 V), which is due to the presence of additional phenyl ring on quinoline and quinoxaline residues.

Carbon dioxide fixation and kinetic studies

The CO_2 fixation reactions were performed using **1** - **5** as a catalyst and one equivalent of sacrificial reducing agent Et_3N in acetonitrile at room temperature.[51,52] The complex **1** shows fixation of atmospheric CO_2 in presence of Et_3N and afforded a blue color solid [Cu(L1)(CO_3)(H_2O)] **(1a)** with a yield of 29 %. However, the efficiency of CO_2 fixation has enhanced on purging pure CO_2 gas under the identical condition and yielded 74 % of **1a**. This CO_3^{2-} bound complex exhibited a completely new absorption band at 614 nm (ε, 362 M^{-1} cm^{-1}) and IR stretching frequency at 1647 cm^{-1} for bound CO_3^{2-}. Further, **1a** was successfully crystallized from the reaction mixture and its molecular structure determined by single-crystal X-ray studies (Figure 4, Table 3 and 4). It shows distorted square pyramidal geometry (τ, 0.369) around copper(II) center via the coordination of only one ligand unit, a carbonate and water molecules. This observation is interesting because one of the ligand

View Article Online
DOI: 10.1039/C7DT03062B

units in the parent complex is replaced by more basic CO_3^{2-} ion (pK_a, 10.2), which is originated from CO_2. However, the addition of one equivalent of H^+ (HCl) to **1a** liberates HCO_3^- and regenerates **1**. The regeneration of **1** is confirmed by the recurrence of ESI-MS, *m/z,* 475.08 and d-d transitions around 776 and 943 nm as similar to the original spectral signatures. Further, the Cu(II)/Cu(I) redox potential of **1a** (0.090 V) is less positive than that of **1** (0.390 V) due to the coordination of better electron donor CO_3^{2-} anion. The CO_3^{2-} coordination is possibly increased the electron density of copper center as compared to the ligand L1. Similarly, the fixation of atmospheric CO_2 by **2** in presence of Et_3N yielded a blue color solid $[Cu(L2)(CO_3)(H_2O)]$ (**2a)**. The observed yield 26% is almost identical to that of **1a**. Whereas, the yield has increased to 73% on purging pure CO_2 gas under identical condition. The absorption band at 650 nm (ε, 295 M^{-1} cm^{-1}) and IR stretching frequency at 1653 cm^{-1} were observed for **2a** as similar to **1a**. The complex **3** has fixed the higher amount of CO_2 in presence of Et_3N and yielded $[Cu(L3)(CO_3)(H_2O)]$ (**3a)** (32% and 81% using atmosphere and pure CO_2 respectively). However, the phenyl substituted complexes **4** and **5** showed a decreased amounts of CO_3^{2-} bound complexes $[Cu(L4)(CO_3)(H_2O)]$ (**4a)** and $[Cu(L5)(CO_3)(H_2O)]$ (**5a)** respectively from the atmosphere (~ 20%) and pure CO_2 (~ 66%) under identical conditions. The IR stretching frequency of bound CO_3^{2-} of **4a** and **5a** appeared almost at similar regions (1649 cm^{-1}). The lower yield of **4a** and **5a** are possibly due to the phenyl groups on **4** and **5** which appears to less facilitate the CO_2 fixation**.** As similar to the observation for **1a**, the Cu(II)/Cu(I) redox potential of **2a** - **5a** are less positive than their respective parent complexes.

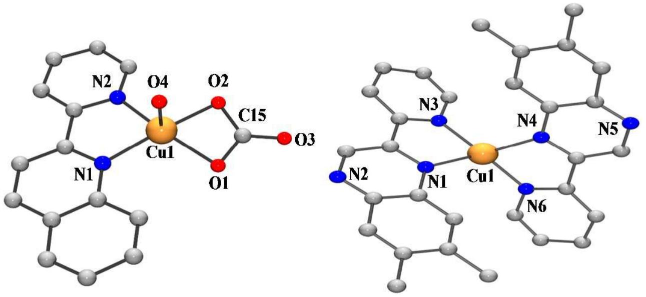

Figure 4. The molecular structures of $[Cu(L1)(CO_3)(H_2O)]$ **1a** and Cu(I)-species $[Cu(L3)_2]ClO_4$ **3b** (Pov-ray figures drawn from 50% probability factor of thermal ellipsoids). The hydrogen atoms, H_2O molecule at outer coordination sphere and perchlorate counter ion are omitted for clarity.

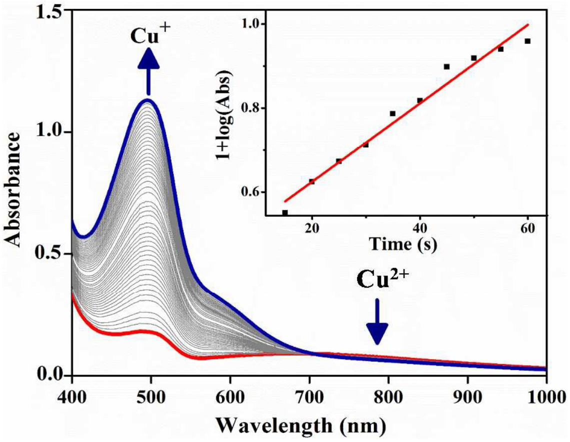

Figure 5. The kinetics of Cu(I)-species formation by the reaction of **1** (1×10^{-3} M) with one equivalent of Et_3N in acetonitrile at 25 ˚C. Inset: plot of [1+log(abs)] vs time.

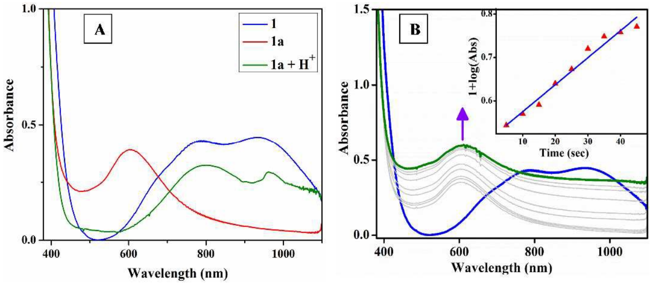

Figure 6. (A) Electronic spectra of **1**, **1a** and **1a** with H^+ (HCl) in acetonitrile at 25 ˚C. (**B)** The kinetic behavior of **1** with CO_2 in the presence of Et_3N at 25 ˚C in acetonitrile. Inset: plot of [1+log(abs)] vs time.

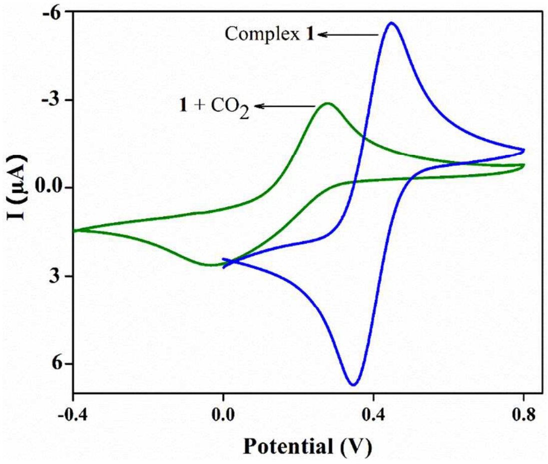

Figure 7. Cyclic Voltammograms of **1** (blue) and **1a** (green) in acetonitrile at 25 °C. Supporting electrolyte: TBAP. Working electrode: Pt sphere, Reference electrode: Ag/Ag^+ (non-aqueous) and counter electrode: Pt wire.

View Article Online
DOI: 10.1039/C7DT03062B

Table 3. Selected bond distances[a] (Å) and bond angles[a] (°) for **1a** and **3b**.

1a		**3b**	
Cu(1)-N(1)	2.014(3)	Cu(1)-N(1)	2.055(3)
Cu(1)-N(2)	1.981(3)	Cu(1)-N(3)	1.993(4)
Cu(1)-O(1)	1.989(2)	Cu(1)-N(4)	2.055(3)
Cu(1)-O(2)	1.959(2)	Cu(1)-N(6)	1.994(4)
Cu(1)-O(4)	2.175(3)		
O(2)-Cu(1)-N(2)	97.96(11)	N(1)-Cu(1)-N(6)	117.15(15)
O(2)-Cu(1)-O(1)	66.83(10)	N(1)-Cu(1)-N(4)	117.37(18)
N(2)-Cu(1)-O(1)	150.85(12)	N(1)-Cu(1)-N(3)	81.45(15)
O(2)-Cu(1)-N(1)	173.01(10)	N(3)-Cu(1)-N(6)	145.6(2)
N(2)-Cu(1)-N(1)	81.89(12)	N(3)-Cu(1)-N(4)	117.15(15)
O(1)-Cu(1)-N(1)	110.16(11)	N(4)-Cu(1)-N(6)	81.45(15)
O(2)-Cu(1)-O(4)	94.46(11)		
N(2)-Cu(1)-O(4)	103.72(12)		
O(1)-Cu(1)-O(4)	102.21(11)		
N(1)-Cu(1)-O(4)	92.36(11)		

[a] Standard deviations in parenthesis

We propose that the CO_2 fixation reaction by **1 - 5** is operating via reduction of copper(II) center into copper(I) by sacrificial one-electron reducing agent Et_3N[51,52] and followed by CO_2 activation as similar to the carbonic anhydrase enzyme.[14-17] The involvement of copper(I) species is spectroscopically monitored and its formation accomplished by an absorption band around 450 - 500 nm. They were generated *in situ* from **1 - 5** by adding one equivalent of Et_3N in acetonitrile at room temperature.[53,54] The complex **1** shows formation of copper(I) species with the rate (k_{obs}) of 9.35×10^{-3} s^{-1} (Figure 5, Table 2) and this rate **1** is almost identical to that of **2** (8.72×10^{-3} s^{-1}) and **3** ($10.31 \times 10^{-3} s^{-1}$). However, a slightly decreased rate of formation has measured for **4** (5.41×10^{-3} s^{-1}) and **5** (5.57×10^{-3} s^{-1}) as due to steric hindrance offered by phenyl groups (Figure S1 – S4). Interestingly, the copper(I) species $[Cu(L3)_2]ClO_4$ (**3b**) of **3** has been crystallized from the reaction mixture. This molecular structure consists of a discrete monomeric unit of a cationic copper(I) complex and a perchlorate anion in the outer coordination sphere. It adopted a distorted tetrahedral geometry by the coordination of two units of ligand L3 (Figure 4, Table 3 and 4). However, the repeated attempts to crystallize copper(I)-species of other complexes were unsuccessful. The reduced copper(I)-species is nucleophilic in nature and subsequently reacts with CO_2 molecule and then finally yielded the corresponding CO_3^{2-} bound complex of type $[Cu(L)(CO_3)H_2O]$. Whereas one of the ligand units is displaced by more basic CO_3^{2-} ion due to its higher pK_a value (10.2) than the ligand heterocycles (pK_a: pyridine, 5.2; quinoline, 4.9; quinoxaline, 0.60).[55-58] A completely distinct CO_3^{2-} to Cu(II) LMCT transition around 614 -673 nm appeared for CO_3^{2-} bound complexes by diminishing of original d-d transitions. The formation kinetics of **1a** has been followed by monitoring the appearance of CO_3^{2-} to copper(II) LMCT band at 614 nm from atmospheric CO_2 in the presence of Et_3N. The calculated rate of formation is 6.22×10^{-3} s^{-1} (Figure 6B, Table 2). Very similar spectral changes have been noted for **2a – 5b** (Figure S6). The treatment of CO_3^{2-} bound complexes with one equivalent of H^+ (HCl) resulted in regeneration of the respective parent copper(II) complexes (Figure 6A) by aerial oxidation[52] or possibly facilitated by H^+ under N_2 atmosphere. Further purging of CO_2 into this solution results in the formation of CO_3^{2-} bound complexes again. The catalysts were active up to eight consecutive cycles and a thereafter slight decrease in efficiency has noted in every subsequent step (Figure S10). The blank reaction without catalyst showed no fixation of atmospheric and pure CO_2 under identical conditions. Also, no CO_2 fixation was observed while using copper(II) complexes as catalyst without sacrificial reducing agent Et_3N. The Et_3N facilitates the one electron reduction of Cu(II) into Cu(I)-species[52] and subsequently CO_2 fixation. The possible oxidation product of Et_3N is Et_3NHClO_4, which was not isolated and characterized in the present study.[52] The involvement of Cu(I)-species in CO_2 fixation have been previously reported by Bouwman and co-workers[23] and Maverick co-workers.[25] However, interestingly, Comba and co-workers have reported the involvement of Cu(II)-species using patellamides ligands.[26] The analogues copper(II) complexes of 2,2'-bipyridine and 1,10-phenanthroline were showed no concomitant CO_2 fixation from the atmosphere and pure CO_2 (Figure S8) under identical conditions. Also, well explored copper(II) complexes $[Cu(BPMN)](ClO_4)_2$ (BPMN=*N,N'*-bis(2-pyridylmethyl)-*N,N'*-dimethylethane-1,2-diamine), $[Cu(iso\text{-}bpmen)](ClO_4)_2$ (*iso*-bpmen=*N,N*-bis(2-pyridylmethyl)-N',N'-dimethylethane-1,2-diamine) were also incapable to fix CO_2 under similar reaction conditions. The reactions were carefully monitored by ESI-MS, electronic spectral and electrochemical methods and exhibited no significant changes in acetonitrile, methanol, and dichloromethane.

View Article Online
DOI: 10.1039/C7DT03062B

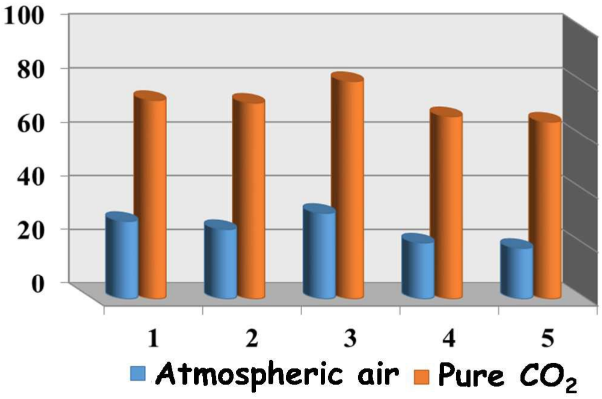

Figure 8. Bar diagram for the yield of carbonate bound complexes **1a – 5a** using pure CO_2 and atmospheric air.

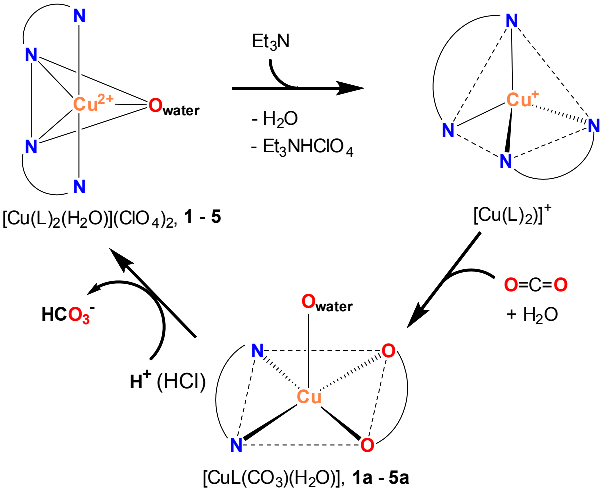

Scheme 2. Fixation of CO_2 by **1 - 5** and their catalytic cycle.

The CO_2 fixation mechanism is possibly proceeded through the geometrical interconversion of trigonal bipyramidal into flattened tetrahedron geometry during the reduction of copper(II) to copper(I) and then to square pyramidal geometry at the product formation stage. These processes have accomplished by loss of the water molecule and slight changes in Cu-N bond distances and followed by the displacement of one of the ligand units by CO_3^{2-} ion. The ligand architecture, donor properties of the heterocyclic nitrogen donors and the enforced structures provide important differences to other catalysts reported. The present ligand systems have the unique ability to provide preferable tetrahedral coordination geometry for stabilization of key copper(I) intermediate and subsequent carbon dioxide fixation. The analogues copper(II) complexes of 2,2'-bipyridine, 1,10-phenanthroline and relevant linear tetradentate N4 ligands were unable to stabilize copper(I)-species for carbon dioxide fixation from the atmosphere and commercial source under identical conditions.

Summary

The copper(II) complexes of new simple bidentate ligands have been synthesized as the catalysts for selective fixation of CO_2 from the atmosphere and were characterized by HR-MS, electronic spectral and redox methods. The single crystal X-ray structure of one the complexes showed an unusual trigonal bipyramid geometry (τ, 0.936) around copper(II) center, which is coordinated by two ligand units and a water molecule. The Cu–N_{quin} bond distances are slightly longer than Cu–N_{pyr} and shorter than Cu-O_{water} bond distances. All these complexes exhibited a well-defined Cu(II)/Cu(I) reduction potentials and the d-d transitions corresponding to a five-coordinate geometry in solution. The rhombic EPR spectra of complexes with three different g values reveal a geometry in between the trigonal bipyramidal and square pyramidal at 70 K. Atmospheric CO_2 has been fixed successfully by present copper(II) complexes using Et_3N as sacrificial reducing agent and yielded the CO_3^{2-} bound complexes of type $[Cu(L)CO_3(H_2O)]$. One of the CO_3^{2-} bound complexes has been crystallized from the reaction mixture and it shows distorted square pyramidal geometry (τ, 0.369) around copper(II) center via the coordination of only one ligand unit, a carbonate and water molecules. The fixation of CO_2 possibly proceeds via the copper(I) species, which is accomplished by the geometrical interconversions. Further, the key copper(I) intermediate of one of the complexes has been crystallized. It showed distorted tetrahedral geometry by the coordination of two units of ligand. The bound carbonate has liberated as HCO_3^- by addition of H^+ and regenerated parent complexes under N_2 atmosphere. The regenerated catalysts were active up to eight consecutive cycles. The catalytic and kinetic studies are showing that fixation of atmospheric CO_2 by the present complexes is selective and simultaneous under mild condition.

Experimental section

Materials

The precursor, 2-aminobenzaldehyde required for the synthesis of target compounds was synthesized by a reduction of 2-nitrobenzaldehyde with iron powder according to a literature procedure.[57] All other chemicals 2-acetylpyridine, 2-nitrobenzaldehyde, 1,2-diaminobenzene, 2-aminobenzophenone, 4,5-dimethylbenzene-1,2-diamine were procured from commercial sources and used as received. Solvents were obtained from commercial suppliers and distilled over suitable drying agents immediately prior to use. All of the ligands were purified by column chromatography using 60-120 mesh silica gel.

Physical measurements: HR-MS was recorded on Agilent 6540 UHD Q-TOF mass spectrometer, FT-IR was recorded on Thermo Nicolet 6700 FT-IR spectrometer. ESI-Mass spectra were recorded on Thermo LC-MS instrument. NMR spectra were recorded by using

View Article Online
DOI: 10.1039/C7DT03062B

300 MHz Bruker instrument. UV-vis spectra were recorded using Agilent diode array spectrometer (Agilent 8453). The EPR spectra of the complexes were recorded on a JEOL JES-TE100 ESR spectrometer operating at X-band frequencies and having a 100 kHz field in MeOH/DMF at liquid nitrogen temperature (70 K). Cyclic voltammetry (CV) was performed using a three-electrode cell configuration (CHI, model 440). A glassy carbon, platinum wire and $Ag(s)/Ag^+$ were used as working, auxiliary and reference electrodes respectively. The supporting electrolyte used was Bu_4NCl. The $E_{1/2}$ values were observed under identical conditions for various scan rates.

X-ray crystal structure analysis

Single crystals of **2**, **3**, and **1a** of suitable size were selected from the mother liquor and immersed in paraffin oil, then mounted on the tip of a glass fibre. Single crystal X-ray diffraction measurements were performed on Agilent Technologies Supernova-E CCD diffractometer. Crystal of complexes was mounted on a STOE image plate diffraction system equipped with a ϕ circle goniometer, using Mo-Kα graphite monochromated radiation (λ = 0.71073 Å). The structures were solved by direct methods using the program SHELXS-2013. Refinement and all further calculations were carried out using SHELXL-2013. The H-atoms were included in calculated positions and treated as riding atoms using the SHELXL default parameters. The non-H atoms were refined anisotropically, using weighted full-matrix least-square on F^2. CCDC 1567430, 1567435 and CCDC 1567437 are containing the supplementary crystallographic data for this paper. These data can be obtained free of charge from The Cambridge Crystallographic Data Centre via www.ccdc.cam.ac.uk/data request/cif.

Synthesis of ligands

2-Pyridin-2-yl-quinoline (L1): Over a solution of 2-nitrobenzaldehyde (1.51 g, 10 mmol) in absolute ethanol (30 mL), iron powder (2.40 g, 40 mmol) and 0.1 M HCl (5 mL) were successively added. The resulting mixture was stirred at 70 °C for 1 h. After consumption of 2-nitrobenzaldehyde monitored by thin layer chromatography, 2-acetyl pyridine (1.20 g, 10.0 mmol) and powdered KOH (0.67 g, 12 mmol) were successively added portion wise. The resulting mixture was vigorously stirred at 80 °C for 3 h. Then, the reaction mixture was allowed to cool down, the excess of iron powder was removed by filtration through a celite pad, and the solvent was evaporated under reduced pressure. Then, the residue was dissolved in dichloromethane, washed with water, dried over anhydrous Na_2SO_4, and concentrated by rotary evaporation. The resulting crude product was subject to silica gel column chromatography eluting with ethyl acetate/n-hexane (1:1) to afford the pure title compound **L1**. White solid (1.45 g, 70 %), mp 90-94 °C; ^1H NMR (400 MHz, *d*-$CDCl_3$) δ 8.67-8.66 (d, 1H, *J* = 4 Hz), 8.61-8.59 (d, 1H, *J* = 8 Hz), 8.50-8.48 (d, 1H, *J* = 8 Hz), 8.22-8.20 (d, 1H, *J* = 8 Hz), 8.14-8.12 (d, 1H, *J* = 8 Hz), 7.82-7.76 (m, 2H), 7.68-7.64 (t, 1H, *J* = 8 Hz), 7.49-7.45 (t, 1H, *J* = 8 Hz), 7.30-7.27 (t, 1H, *J* = 6 Hz). ESI-MS: *m/z* = 207 (M^+).

Table 4. Crystal data and structure refinement for $[Cu(L2)_2(H_2O)](H_2O)(ClO_4)_2$ **2,** $[Cu(L1)(CO_3)(H_2O)]$ $3(H_2O)$ **1a** and $[Cu(L3)_2](ClO_4)$ **3b**.

	2	**1a**	**3b**
Formula	$CuC_{26}H_{20}Cl_2N_6O_{10}$	$CuC_{15}H_{18}N_2CuO_7$	$CuC_{30}H_{26}ClN_6O_4$
Fw	702.92	401.85	633.56
Crystal system	Tetragonal	Triclinic	Monoclinic
Space group	I 41/a	P -1	C 2/c
Temperature	297.4(4)	295(1)	295.9(7)
a/Å	20.7098(11)	8.0993(6)	14.5802(11)
b/Å	20.7098(11)	10.3092(6)	14.7784(8)
c/A^0	27.0998(16)	11.0759(8)	14.3077(11)
α/^{0}	90	96.292(5)	90
β/^{0}	90	107.070(7)	114.588(9)
γ/^{0}	90	108.306(6)	90
Volume/Å^3	11623.0(14)	818.32(11)	2803.4(4)
Z	16	2	4
ρ_{calc}mg/mm^3	1.607	1.631	1.501
μ/mm^{-1}	1.001	1.376	0.923
F(000)	5712	414	1304
Reflection collected	14288	5194	6239
Goodness-of-fit on F^2	1.032	1.059	1.022
R1[a]	0.0858	0.0537	0.0757
wR2[b]	0.2926	0.1333	0.2349

[j]$R1=\sum||F_o|-|Fc||/\sum|F_o|$,[k]$R_2=\sum w[(F_o-F_c)^2/\sum w[(F_o^2)^2]^{1/2}$

View Article Online
DOI: 10.1039/C7DT03062B

2-Pyridin-2-yl-quinoxaline (L2): 1, 2-Diaminobenzene (1.62 g, 15 mmol) and 2-acetylpyridine (1.81 g, 15 mmol) were added to a 100 mL round-bottom flask with methanol (20 mL). Silica gel (60-120 mesh, 0.05 g and HCl 10 %, 2 mL) were added sequentially to the round-bottom flask, resulting solution was heated at reflux (85 °C) for 24 h under argon atmosphere. The reaction was then cooled to room temperature, diluted with water and neutralized with 10 % Na_2CO_3 (50 mL). It was extracted with chloroform (3 × 100 mL). The extract was washed with water and dried over anhydrous Na_2SO_4. The chloroform was removed under reduced pressure and the remaining crude product was purified by flash column chromatography on silica gel (n-hexane: EtOAc). White solid (2.4 g, 80 %), mp 88-90 °C; ^{1}H NMR (400 MHz, *d*-$CDCl_3$) δ 9.90 (s, 1H), 8.73-8.72 (d, 1H, *J* = 4 Hz), 8.55-8.53 (d, 1H, *J* = 8 Hz), 8.11-8.09 (d, 2H, *J* = 8 Hz), 7.86-7.82 (t, 1H, *J* = 8 Hz), 7.74-7.72 (t, 1H, *J* = 6 Hz), 7.37-7.34 (t, 1H, *J* = 6 Hz), 6.97-6.94 (d, 1H, *J* = 12 Hz). ESI-MS: *m/z* = 208 (M^+).

6,7-Dimethyl-2-pyridin-2-yl-quinoxaline (L3): Using the similar method for compound L2, compound L3 was prepared by reaction of 2-acetylpyridine (1.81 g, 15 mmol) and 4, 5-dimethylbenzene-1,2-diamine (2.04 g, 15 mmol) in anhydrous methanol. Orange solid (2.04 g, 58 %), mp 162-164 °C; ^{1}H NMR (400 MHz, *d*-$CDCl_3$) δ 9.77 (s, 1H), 8.70-8.69 (d, 1H, *J* = 4 Hz), 8.49-8.47 (d, 1H, *J* = 8 Hz), 7.83-7.80 (t, 3H, *J* = 6 Hz), 7.33-7.30 (t, 1H, *J* = 6 Hz), 2.44 (s, 6H). ESI-MS: *m/z* = 236 (M^+).

4-Phenyl-2-pyridin-2-yl-quinoline (L4): To a Schlenk flask containing 2-aminobenzophenone (2.95 g, 15 mmol) in dry acetic acid (20 mL) and con. H_2SO_4 (0.3 mL) were added 2-acetylpyridine (2.0 g, 16.5 mmol). After the flask was flushed with nitrogen, it was stirred at 140 °C under an atmosphere of nitrogen for 12 h. Upon completion of the reaction, it was quenched with saturated ammonia/ice mixture and extracted with $CHCl_3$ (50 mL × 3). The combined organic phases were dried over anhydrous Na_2SO_4 and concentrated under vacuum. The residue was purified by column chromatography on silica gel with petroleum ether/ethyl acetate (2:1) as eluent to give L4. Pale yellow solid (2.75 g, 65 %), mp 150-154 °C; ^{1}H NMR (400 MHz, *d*-$CDCl_3$) δ 8.73-8.69 (m, 2H), 8.52 (s, 1H), 8.26-8.24 (d, 1H, *J* = 8 Hz), 7.97-7.95 (d, 1H, *J* = 8 Hz), 7.91-7.87 (t, 1H, *J* = 8 Hz), 7.76-7.73 (t, 1H, *J* = 6 Hz), 7.59-7.49 (m, 5H), 7.36-7.34 (t, 2H, *J* = 4 Hz). ESI-MS: *m/z* = 283 (M^+).

4-Phenyl-2-pyridin-2-yl-quinazoline (L5): 2-Aminobenzophenone (1.97 g, 10 mmol) and 2-pyridinecarboxaldehyde (1.07 g, 10 mmol), ammonium acetate (1.0 g, 13 mmol) and iodine (0.05 g, 0.2 mmol) were added to a 100 mL round-bottom flask with ethanol (30 mL). The resulting mixture was heated at 50 °C for 5 h. The mixture was cooled to room temperature, and the resulting mixture was evaporated to dryness. The resulting solid was washed with water and extracted with $CHCl_3$. The combined organic phases were dried over anhydrous Na_2SO_4 and concentrated under vacuum. The residue was purified by column chromatography on silica gel with petroleum ether/ethyl acetate (2:1) as eluent to give L5. Brown solid (1.27 g, 45 %), mp 164 - 168 °C; ^{1}H NMR (400 MHz, *d*-$CDCl_3$) δ 8.94-8.93 (d, 1H, *J* = 4Hz), 8.79-8.77 (d, 1H, *J* = 8 Hz), 8.39-8.37 (d, 1H, *J* = 8Hz), 8.18-8.16 (d, 1H, *J* = 8 Hz), 7.96-7.90 (m, 4H), 7.64-7.60 (t, 4H, *J* = 6Hz), 7.44-7.41 (t, 1H, *J* = 8Hz). ESI-MS: *m/z* = 284 (M^+).

Synthesis of Cu(II) complexes 1-5

Caution! During handling of the perchlorate salts of metal complexes with organic ligands, care should be taken because of the possibility of explosion.

$[Cu(L1)_2(H_2O)](ClO_4)_2$ (1): To a stirred solution of L1 (0.21 g, 1.0 mmol) in MeOH (15 mL) was added dropwise to a MeOH solution of (10 mL) $Cu(ClO_4)_2.6H_2O$ (0.19 g, 0.5 mmol). The mixture was stirred for 3 h, during which a green precipitate was formed. This was filtered off, washed with cold MeOH and then dried under vacuum. Yield, 0.55 g (82 %). HR-MS (*m/z*): calculated for $C_{28}H_{20}CuN_4$ $[M]^+$ 475.0984; found 475.0989.

The other complexes **2** – **5** have been also synthesized by the above-described method under identical reaction condition.

$[Cu(L2)_2(H_2O)](ClO_4)_2$ (2): Isolated as green solid and yield is 0.21 g (94%). Confirmed by HR-MS (*m/z*): calculated for $C_{26}H_{18}CuN_6$ $[M]^+$ 477.0889; found 477.0899.

$[Cu(L3)_2(H_2O)](ClO_4)_2$, (3): It is a brown solid with the yield of 0.15 g (87%). Confirmed by HR-MS (*m/z)*: calculated for $C_{30}H_{26}CuN_6$ $[M]^+$ 533.1515; found 533.0563.

$[Cu(L4)_2(H_2O)](ClO_4)_2$ (4): Yellow color solid has been isolated with a yield of 0.10 g (83%). Confirmed by HR-MS (*m/z*): calculated for $C_{40}H_{28}CuN_4$ $[M]^+$ 627.1610; found 627.1824.

$[Cu(L5)_2(H_2O)](ClO_4)_2$ (5): Dark green solid was isolated and the yield is 0.10 g (81%). Conformed HR-MS (*m/z*): calculated for $C_{38}H_{26}CuN_6$ $[M]^+$ 629.1515; found 629.1521.

Carbon dioxide fixation studies

A solution of Cu(II) complexes (0.5 mmol) in 5mL acetonitrile was treated with one equivalent of sacrificial reducing agent Et_3N to affords Cu(I)-complexes. Then, the solution was purged with atmospheric air/pure CO_2 at room temperature to afford blue

View Article Online
DOI: 10.1039/C7DT03062B

coloured crystalline solid [Cu(L)(CO_3)(H_2O)]. Recrystallization of these solids from acetonitrile afforded blue colored crystals suitable for X-ray crystallographic analysis. Further, the formation of CO_3^{2-} complexes confirmed by the appearance of electronic absorption bands around 614 nm and IR stretching frequency for CO_3^{2-} around 1647 cm^{-1}.

Kinetic studies

Kinetic experiments of the copper(I) species formation were studied by spectrophotometrically as time-dependent measurement at 25 ^{o}C. The intermediate [Cu(L)]$^{+}$ species were generated by treating the stoichiometric amount of complexes (1 × 10^{-3} M) with an equivalent amount of sacrificial reducing agent Et_3N (1 × 10^{-3} M) in acetonitrile. After the kinetics, the reaction mixtures were kept for crystallization by slow evaporation at room temperature and suitable crystals were used for single crystal X-ray studies.

Conflicts of interest

The authors declare no conflicts of interest.

Acknowledgement

We acknowledge Science and Engineering Research Board (SERB), New Delhi and Board of Research in Nuclear Science (BRNS), Mumbai for funding.

References

1 M. Aresta, A. Dibenedetto, A. Angelini, *Chem. Rev.,* 2014, **114**, 1709-1742.

2 A. S. Lindsey, H. Jeskey, *Chem. Rev.,* 1957, **57** , 583-620.

3 S. M. Glueck, S. Gumus, W. M. F. Fabian, K. Faber, *Chem. Soc. Rev.,* 2010, **39**, 313-328.

4 C. K. Savile, J. J. Lalonde, *Curr. Opin. Biotechnol.,* 2011, **22**, 818-823.

5 W. Wang, S. Wang, X. Ma, J. Gong, *Chem. Soc. Rev.,* 2011, **40**, 3703-3727.

6 E. V. Kondratenko, G. Mul, J. Baltrusaitis, G. O. Larrazabal, J. Perez-Ramirez, *Energy Environ. Sci.,* 2013, **6**, 3112-3135.

7 A. M. Appel, J. E. Bercaw, A. B. Bocarsly, H. Dobbek, D. L. DuBois, M. Dupuis, J. G. Ferry, E. Fujita, R. Hille, P. J. A. Kenis, C. A. Kerfeld, R. H. Morris, C. H. F. Peden, A. R. Portis, S. W. Ragsdale, T. B. Rauchfuss, J. N. H. Reek, L. C. Seefeldt, R. K. Thauer, G. L. Waldrop, *Chem. Rev.,* 2013, **113**, 6621-6658.

8 H. Arakawa, M. Aresta, J. N. Armor, M. A. Barteau, E. J. Beckman, A. T. Bell, J. E. Bercaw, C. Creutz, E. Dinjus, D. A. Dixon, K. Domen, D. L. DuBois, J. Eckert, E. Fujita, D. H. Gibson, W. A. Goddard, D. W. Goodman, J. Keller, G. J. Kubas, H. H. Kung, J. E. Lyons, L. E. Manzer, T. J. Marks, K. Morokuma, K. M. Nicholas, R. Periana, L. Que, J. Rostrup-Nielson, W. M. H. Sachtler, L. D. Schmidt, A. Sen, G. A. Somorjai, P. C. Stair, B. R. Stults, W. Tumas, *Chem. Rev.,* 2001, **101**, 953-996.

9 A. Behr, *Angew. Chem., Int. Ed. Engl.,* 1988, **27**, 661-678.

10 M. Aresta, A. Dibenedetto, *Dalton Trans.,* 2007, 2975-2992.

11 P. G. Jessop, T. Ikariya, R. Noyori, *Chem. Rev.,* 1995, **95**, 259-272.

12 Y. Oh, X. Hu, *Chem. Soc. Rev.,* 2013, **42**, 2253-2261.

13 P. A. Lindahl, *Biochemistry* 2002, **41**, 2097-2105.

14 P. Woolley, *Nature* 1975, **258**, 677-682.

15 K. M. Merz, R. Hoffmann, M. J. S. Dewar, *J. Am. Chem. Soc.,* 1989, **111**, 5636-5649.

16 V. M. Krishnamurthy, G. K. Kaufman, A. R. Urbach, I. Gitlin, K. L. Gudiksen, D. B. Weibel, G. M. Whitesides, *Chem. Rev.,* 2008, **108**, 946-1051.

17 A. E. Eriksson, T. A. Jones, A. Liljas, *Proteins.,* 1988, **4**, 274-282.

18 A. Schrodt, A. Neubrand, R. van Eldik, *Inorg. Chem.,* 1997, **36**, 4579-4584.

19 T. Tanase, S. Nitta, S. Yoshikawa, K. Kobayashi, T. Sakurai, S. Yano, *Inorg. Chem.,* 1992, **31**, 1058-1062.

20 E. Kimura, *Acc. Chem. Res.,* 2001, **34**, 171-179.

21 L. J. Farrugia, S. Lopinski, P. A. Lovatt, R. D. Peacock, *Inorg. Chem.,* 2001, **40**, 558-559.

22 E. Garcia-Espana, P. Gavina, J. Latorre, C. Soriano, B. Verdejo, *J. Am. Chem. Soc.,* 2004, **126**, 5082-5083.

23 R. Angamuthu, P. Byers, M. Lutz, A. L. Spek, E. Bouwman, *Science* 2010, **327**, 313.

24 H. Takisawa, Y. Morishima, S. Soma, R. K. Szilagyi, K. Fujisawa, *Inorg. Chem.,* 2014, **53**, 8191-8193.

25 U. R. Pokharel, F. R. Fronczek, A. W. Maverick, *Nat. Commun.,* 2014, **5**, 5883.

26 P. Comba, L. R. Gahan, G. R. Hanson, M. Maeder, M. Westphal, *Dalton Trans.,* 2014, **43**, 3144-3152.

27 S. S. Massoud, F. R. Louka, M. A. Al-Hasan, R. Vicente, F. A. Mautner, *New. J. Chem.,* 2015, **39**, 5944-5952.

28 A. H. Li, E. Ahmed, X. Chen, M. Cox, A. P. Crew, H. Q. Dong, M. Jin, L. Ma, B. Panicker, K. W. Siu, A. G. Steinig, K. M. Stolz, P. A. R. Tavares, B. Volk, Q. Weng, D. Werner, M. J. A. Mulvihill, *Org. Biomol. Chem.,* 2007, **5**, 61-64.

29 S. J. Stoessel, C. M. Elliott, J. K. Stille, *Chem. Mater.,* 1989, **1**, 259-268.

30 D. I. Jung, J. H. Song, Y. H. Kim, D. H. Lee, Y. G. Lee, Y. M. Park, S. K. Choi, J. T. Hahn, *Bull. Korean Chem. Soc*., 2007, **28**, 1877-1880.

31 S. K. Panja, N. Dwivedi, S. Saha, *Tetrahedron. Lett.,* 2012, **53**, 6167-6172.

32 (a) M. Palaniandavar, I. Somasundaram, M. Lakshminarayanan, H. Manohar, *J. Chem. Soc., Dalton Trans.,* 1996, 1333-1340; (b) U. Sakaguchi, A. W. Addison, *J. Chem. Soc., Dalton Trans.,* 1979, 600-608; (c) J. E. Huheey, E. Keiter, R. L. Keiter, O. K. Medhu, *Inorganic Chemistry, Principles of Structure and Reactivity*, Pearson Education, Upper Saddle River, NJ, 2006, 425–426.

33 A. W. Addison, T. N. Rao, J. Reedijk, J. van Rijn, G. C. Verschoor, *J. Chem. Soc., Dalton Trans.,* 1984, **7**, 1349-1356.

34 G. Murphy, C. Murphy, B. Murphy, B. Hathaway, *J. Chem. Soc., Dalton Trans.,* 1997, 2653-2660.

View Article Online
DOI: 10.1039/C7DT03062B

35 P. Nagle, E. O'Sullivan, B. J. Hathaway, E. Muller, *J. Chem. Soc., Dalton Trans.,* 1990, 3399-3406.

36 S. Muthuramalingam, S. Subramaniyan, T. Khamrang, M. Velusamy, R. Mayilmurugan, *ChemistrySelect* 2017, **2**, 940-948.

37 Y. Yao, M. W. Perkovic, D. P. Rillema, C. Woods, *Inorg. Chem.,* 1992, **31**, 3956-3962.

38 M. Duggan, N. Ray, B. Hathaway, G. Tomlinson, P. Brint, K. Pelin, *J. Chem. Soc., Dalton Trans.,* 1980, 1342-1348.

39 B. J. Hathaway, *in Comprehensive Coordination Chemistry*, ed. G. Wilkinson, R. D. Gillard, J. A. McCleverty, Pergamon Press, Oxford, England, 1987, **5**, 533.

40 S. S. Massoud, F. R. Louka, R. N. David, M. J. Dartez, Q. L. Nguyn, N. J. Labry, R. C. Fischer, F. A. Mautner, *Polyhedron* 2015, **90**, 258-265.

41 S. S. Massoud, L. L. Quan, K. Gatterer, J. H. Albering, R. C. Fischer, F. A. Mautner, *Polyhedron* 2012, **31**, 601-606.

42 W. Xu, J. A. Craft, P. R. Fontenot, M. Barens, K. D. Knierim, J. H. Albering, F. A. Mautner, S. S. Massoud, *Inorg. Chim. Acta* 2011, **373**, 159-166.

43 U. Mukhopadhyay, I. Bernal, S. S. Massoud, F. A. Mautner, *Inorg. Chim. Acta* 2004, **357**, 3673-3682.

44 D. Kivelson, R. Neiman, *J. Chem. Phys*., 1961, **35**, 149.

45 D. Getz, B. L. Silver, *J. Chem. Phys.,* 1974, **61**, 630-637.

46 B. J. Hathaway, D. E. Billing, *Coord. Chem. Rev.,* 1970, **5**, 143-207.

47 P. F. Rapheal, E. Manoj, M. R. Prathapachandra Kurup, *Polyhedron* 2007, **26**, 818-828.

48 B. J. Hathaway, A. A. G. Tomlinson, *Coord. Chem. Rev.,* 1970, **5**, 1-43.

49 (a) H. Nakai, Y. Noda, *Bull. Chem. Soc. Jpn.,* 1978, **51**, 1386-1390; (b) H. Nakai, Y. Deguchi, *Bull. Chem. Soc. Jpn.,* 1975, **48**, 2557-2560; (c) E. Garribba, G. Micera, *J. Chem. Educ.* 2006, **83**, 1229; (d) B. J. Hathaway, *Struct. Bonding* 1984, **57**, 55.

50 Z. M. Wang, H. K. Lin, Z. F. Zhou, M. Xu, T. F. Liu, S. R. Zhu, Y. T. Chen, *Bioorg. Med. Chem.,* 2001, **9**, 2849-2855.

51 (a) H. Yin, Y. Wada, T. Kitamura, S. Yanagida, *Environ. Sci. Technol.* 2001, **35**, 227-231; (b) J. Xie, C. Li, Q. Zhou, W. Wang, Y. Hou, B. Zhang, X. Wang, *Inorg. Chem.* 2012, **51**, 6376-6384; (c) Y. P. Sun, B. Ma, G. E. Lawson, *Chem. Phys. Lett.* 1995, **233**, 57-62; (d) P. K. Singh, S. Nath, A. C. Bhasikuttan, M. Kumbhakar, J. Mohanty, S. K. Sarkar, T. Mukherjee, H. Pal, *J. Chem. Phys.,* 2008, **129**, 114504; (e) S. Prashanthi, P. H. Kumar, L. Wang, A. K. Perepogu, P. R. Bangal, *J. Fluoresc.* 2010, **20**, 571-580; (f) T. Kurahashi, *Inorg. Chem.,* 2015, **54**, 8356-8366; (g) H. Görner, *J. Photochem. Photobiol.,* 2008, **195**, 235-241.

52 J. T. Yoke, J. F. Weiss, G. Tollin, *Inorg. Chem.,* 1963, **2**, 1210-1216.

53 M. Meyer, A. M. Albrecht-Gary, C. O. Dietrich-Buchecker, J. P. Sauvage, *Inorg. Chem.* 1999, **38**, 2279-2287.

54 G. Sanna, M. I. Pilo, M. A. Zoroddu, R. Seeber, S. Mosca, *Inorg. Chim. Acta* 1993, **208**, 153-158.

55 E. A. Braude, F. C. Nachod, W. D. Phillips. *Determination of organic structures by physical methods. New York: Academic press*, 1995-1973.

56 R. Linnell, *J. Org. Chem.,* 1960, **25**, 290-290.

57 R. G. Pearson, F. V. Williams, *J. Am. Chem. Soc.,* 1953, **75**, 3073-3075.

58 C. Zhang, C. Kanta De, D. Seidel, *Org. Synth.,* 2012*,* **89**, 274-282

View Article Online
DOI: 10.1039/C7DT03062B

Table of Contents Graphic and Synopsis

Catalytic fixation of atmospheric carbon dioxide by copper(II) complexes of bidentate ligands

Sethuraman Muthuramalingam,[a] Themmila Khamrang,[b] Marappan Velusamy,*,[b] and Ramasamy Mayilmurugan*,[a]

The copper(II) complexes of simple bidentate ligands have been synthesized and characterized as the catalysts for selective fixation and sequestration of CO_2 from the atmospheric air. The fixation of CO_2 proceeds via the formation of copper(I) species generated by sacrificial reducing agent Et_3N and afforded CO_3^{2-} bound complexes. This CO_2 fixation reaction is accomplished through geomentrical interconversion of trigonal bipyramidal into square pyramidal geometry via tetrahedral Cu(I)-species.

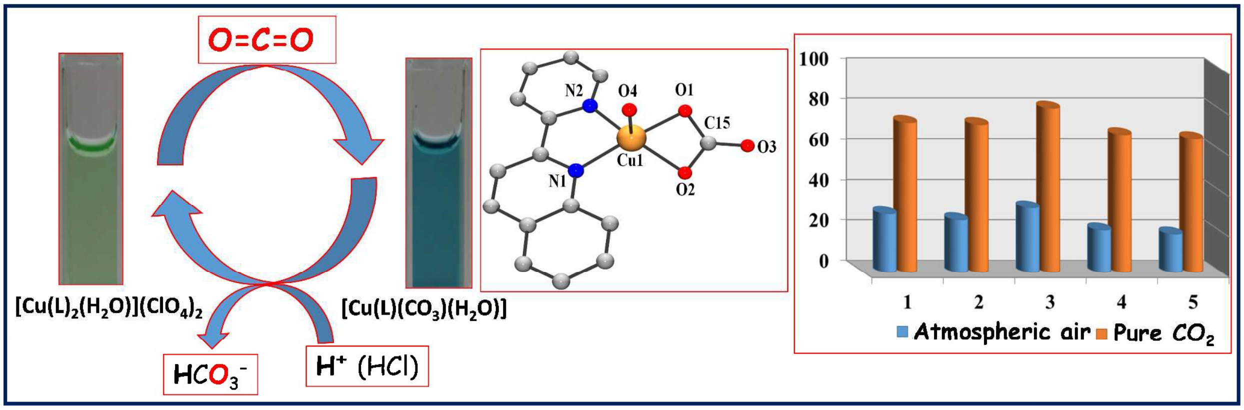

View Article Online
DOI: 10.1039/C7DT03062B